Australian Government
Department of Defence
Defence Science and
Technology Organisation

Assessment of the Effect of Pitting Corrosion on the Safe Life Prediction of the P-3C

A. Shekhter, C. Loader, W. Hu and B. R. Crawford

Air Vehicles Division
Defence Science and Technology Organisation

DSTO-TR-2080

ABSTRACT

This report presents the results of an experimental programme aimed at assessing the implications of pitting corrosion damage on P-3C safe lives calculated using the methods developed in the P-3C Service Life Assessment Program, the Equivalent Crack Size method and the Crack Initiation method. The results of both of these methods were that, for the pitting corrosion distribution used, the safe life prediction was not invalidated by corrosion. However, larger corrosion pits or a change of corrosion mechanism may invalidate safe life predictions.

RELEASE LIMITATION

Approved for public release

Published by

Air Vehicles Division
DSTO Defence Science and Technology Organisation
506 Lorimer St
Fishermans Bend, Victoria 3207 Australia

Telephone: (03) 9626 7000
Fax: (03) 9626 7999

AR-014-063
December 2007

APPROVED FOR PUBLIC RELEASE

Assessment of the Effect of Pitting Corrosion on the Safe Life Prediction of the P-3C

Executive Summary

This report presents the results of an experimental programme aimed at assessing the implications of pitting corrosion damage on P-3C safe lives calculated using the method developed in the P-3C Service Life Assessment Program. Corrosion is known to reduce fatigue life but whether this effect is structurally significant is uncertain. Therefore, high Kt specimens of 7075-T6 were fatigue tested using spectrum loading in corroded and un-corroded states. The data obtained from these tests were analysed in two ways. These were the equivalent crack size method and the crack initiation method developed in the P-3C Service Life Assessment Program.

The equivalent crack size distribution was determined using the fatigue life data obtained from testing, fractographic data collected from scanning electron microscopy and fatigue crack growth rates prediction using FASTRAN. A probabilistic approach was employed to determine a relationship between a measured corrosion metric and an Equivalent Crack Size, which was calculated using the P-3C SLAP safe life approach. Using this method, it was found that pitting corrosion did not reduce fatigue lives below the safe life values. However, it was not possible to determine, given the limited number of tests conducted, a statistical level of confidence for this statement.

Evaluation of the effect of corrosion using the crack initiation method developed in the P-3C Service Life Assessment Program also showed that pitting corrosion did not reduce the fatigue life below the safe life values predicted using the P-3C SLAP method. Based on FASTRAN modelling, pitting corrosion was found to have reduced the time to crack initiation by 26%. The percentage change in initiating crack length due to corrosion was only 0.2%, which suggests that this method has limited sensitivity in this application.

In summary, both the equivalent crack size and crack initiation methods indicated that pitting corrosion did not invalidate the safe life estimates of fatigue life with the given distribution of corrosion pit sizes. In contrast, larger corrosion pits or a different mode of corrosion (i.e. exfoliation) may invalidate safe life estimates.

Authors

Dr. Alexandra Shekhter
Air Vehicles Division

Dr. Alexandra Shekhter, Research Scientist, gained her PhD from Monash University in 2003. She worked in the Department of Materials Engineering at Monash University as a research fellow for two years working on the microstructure and properties of maraging steels. Since commencing in DSTO's Air Vehicles Division in November 2002, she has been involved in long range research focussing on emerging materials technologies for airframes. She has also worked on the certification of Retrogression and Reaging for use on ADF aircraft and on technical risk assessments for novel materials and technologies for new platform acquisitions.

Mr. Christopher Loader
Air Vehicles Division

Christopher Loader, Science and Technology Officer, graduated from Monash University in 1998 with a Bachelor of Science majoring in Chemistry and Materials Science and a Bachelor of Engineering with Honours in Materials Engineering. Since arriving at DSTO in 1998, he has worked on several programs aimed at better understanding corrosion-initiated fatigue in a variety of aluminium and steel alloys used in the aircraft industry. This includes the SICAS project, a major collaborative project between DSTO, CSIRO and BAE Systems, which successfully developed a means of quantifying the effects of pitting corrosion damage on airframe structural integrity.

Chris is currently a task manager and is assessing several novel technologies for use in future and current ADF air platforms. These include comparative vacuum sensors for crack detection and the certification of retrogression re-aging techniques for improving the corrosion resistance of in-service and replacement aircraft components.

Dr. Weiping Hu
Air Vehicles Division

Dr. Weiping Hu joined DSTO in 1998 as a Research Scientist. He is currently a Senior Research Scientist leading the development of modelling capabilities for the analysis of structural integrity of aircraft structures. After obtaining his PhD degree in 1993 at Dublin City University, Ireland, he held various academic positions at Dublin City University, Monash University and Deakin University. His current research interests include fatigue and fracture of engineering materials and structures, fatigue crack growth in aircraft structures, constitutive models and plasticity, and numerical methods in engineering.

Dr. Bruce Crawford
Air Vehicles Division

Dr. Bruce Crawford, Senior Research Scientist, graduated from Monash University in 1991 with a Bachelor of Enginnering in Materials Engineering with first class honours. He subsequently completed a Doctor of Philosophy at the University of Queensland in the field of the fatigue of metal matrix composite materials. Bruce then lectured materials science and engineering for four years at Deakin University in the School of Engineering and Technology before joining DSTO Airframes and Engines Division in 1999. Since joining DSTO Bruce has worked on the development of deterministic and probabilistic model of corrosion-fatigue and structural integrity management for aerospace aluminium alloys.

Contents

1. Introduction

This report describes the development of an Equivalent Crack Size (ECS) distribution from fatigue life and fractographic data obtained from testing the aluminium alloy 7075-T6, which is the principal structural alloy of the P-3C Orion. This distribution was developed using a load spectra from the P-3C Service Life Assessment Program (SLAP). Fatigue specimens with a high stress concentration, representative of fatigue critical regions in the P-3C, were used. This research was conducted in response to a request from the RAAF for an assessment of the impact of pitting corrosion on the structural integrity of the P-3C empennage. The two fundamental questions this reports aims to answer are:

- What are the implications of corrosion for the P-3C SLAP?
- Does corrosion invalidate the current life assessment methodology for the P-3C?

These questions were addressed through the fatigue testing of corroded coupons of aluminium alloy 7075-T6 combined with both statistical and fatigue crack growth analyses. Two approaches were used to predict the effect of corrosion on fatigue life. The first of these was the Equivalent Crack Size approach developed in previous DSTO work [1, 2]. The second was the Crack Initiation (CI) method developed as part of the P-3C SLAP Program [3].

2. Background

2.1 Corrosion in Aircraft Structures

The last few decades have seen a steady increase in the average age of aircraft fleets worldwide due to the enormous cost of replacing aircraft. Therefore, rather than being replaced at the originally scheduled service life, aircraft are being retained for many years longer than their design life. Examples of this include the RAAF F-111 and P-3C Orion.

The retention of aircraft in this manner has not been without consequence. While it has delayed the cost of new acquisitions, the cost of aircraft maintenance increases steadily through life [4]. This is due in part to environmental effects such as the corrosion of metallic parts and the degradation of polymeric components, which were not considered or even known of during the design phase. Corrosion and the attendant loss of structural integrity have caused at least one major air incident, the in-flight disintegration of the upper lobe of the fuselage of an Aloha Airlines 737 [5], and any number of less severe failures such as the loss of the trailing edge flap from F/A-18 Hornets in both Australian and American use [6]. The US Navy has observed failures due to corrosion in numerous aircraft including the F/A-18, P-3, C-130 and the F5 [7]. An analysis by Hoeppner *et al.* of FAA, NTSB and United States military aircraft accident and incident reports showed that corrosion was implicated in between 10 to 16% of the accidents reported [8].

The most dangerous forms of corrosion are pitting, exfoliation and stress corrosion cracking. These are far more insidious than general corrosion as they tend to occur in very small areas and are difficult to detect while still having significant effects on structural integrity. The Aloha Airlines 737 [5] and F/A-18 trailing edge flap failures [6] were fatigue failures attributed to cracks which had initiated from corrosion pits.

In addition to its effects on aircraft safety, corrosion significantly increases the maintenance required on aged airframes. This is primarily because there is no currently accepted way of incorporating the management of corrosion damage into aircraft structural integrity management [9, 10]. Therefore, the policy of many air fleet operators has been 'find and fix'. That is, corrosion damage is removed immediately upon detection. This, of course, removes the aircraft from service while corrosion repairs are being undertaken. In addition to the maintenance cost, the lack of aircraft availability also has a cost both economically and operationally. As a result, an alternative to the 'find and fix' policy could lead to significantly reduced ownership cost, increased fleet safety and reduced maintenance. Such an alternative policy, which was first suggested by Cole *et al.* in 1997 [5], was labelled 'Anticipate and Manage' by Peeler and Kinzie [9]

Analysis of the impact of corrosion and the actions taken as a result of this analysis requires new technologies. These are required so that decisions to repair, replace or retire can be made using a structured and rational framework that allows the demands of safety and structural integrity to be balanced with those imposed by economic pressures. One potential technology that can be used in developing such a framework is the ECS approach examined here. This approach is explained in §3.2.

2.2 P-3C SLAP Program

The work described in this report was an adjunct to the P-3C Service Life Assessment Program. In late 1998 the Royal Australian Air Force (RAAF) entered into the USN P-3C Service Life Assessment Program (SLAP) with the United States Navy (USN), Canada and the Netherlands. This program consists of a Full-Scale Fatigue Test (FSFT) and subsequent teardown of a P-3C airframe. It aims to provide structural clearance in RAAF service of the P-3C airframe to at least 2015. Australia contributed to the P-3C SLAP by conducting a P-3C empennage FSFT at the Defence Science and Technology Organisation (DSTO), providing P-3C flight test loads, P-3C SLAP test interpretation and a P-3C wing teardown. The Australian empennage FSFT involved the testing of an empennage representative of existing RAAF P-3C aircraft to approximately 30,000 Simulated Flying Hours (SFH). In addition, the RAAF has tasked DSTO to translate all the P-3C SLAP fatigue tests into equivalent RAAF fleet usage. This requires the use of analytical fatigue life and crack growth programs that traditionally require some level of verification using the spectra, materials and stress levels particular to the aircraft. This verification usually involves performing coupon tests for both fatigue life and fatigue crack growth. As part of their contributions, Lockheed Martin Aeronautics (LMA), the Canadian Forces (CF) and the National Aerospace Laboratory (NLR) conducted numerous coupon tests. Despite this, it was necessary for DSTO to perform some additional coupon tests specifically directed at supporting the RAAF test interpretation effort. This work is detailed in Reference [3]. The work reported here extends this earlier work as it uses the same materials, coupon geometry and assumption as by DSTO's P-3C SLAP team.

3. Analytical Methods

In this report the fatigue and fractography data obtained from the corroded and uncorroded specimens are analysed using two methods. These are as follows:

1. The CI method developed by DSTO's P-3C SLAP team [3], and
2. The ECS method developed during the SICAS[1] project [1, 2].

The purpose of this dual analysis is to allow comparison of the two methods thereby highlighting the strengths and weaknesses of each in dealing with the effects of corrosion on structural integrity.

3.1 P-3C SLAP Crack Initiation Approach[2]

A test interpretation methodology for the RAAF P-3C fleet has been developed to ensure that the results from the P-3C SLAP will enable the RAAF to continue to maintain the airworthiness and durability of their P-3C aircraft. To achieve this, a balance must be struck between airworthiness and durability [11].

The P-3C SLAP safe life assessment methodology defines component safe lives, inspection thresholds and intervals and other limits such as the onset of Widespread Fatigue Damage. The P-3C SLAP includes a description of all fatigue cracking sites, crack orientations and an estimation of the criticality of each, the definition of the point of 'crack initiation' as well as total fatigue life, crack growth curves and the definition of critical crack lengths. The crack initiation and total fatigue lives are required in order to generate the safe life or inspection-free service lives and the crack growth data are required so that the total crack growth life and the time (in flight hours) at which cracks should be inspected can be determined.

The initial Lockheed-Martin (LM) approach was to set a 'damage initiation' life H_{init} as 2/3 of the life at which a crack was found on the test. The intent of this approach seems to be to ensure that there is a minimum scatter factor of three on test-demonstrated total life to the safe life [3], as a factor of two is already applied. This approach, however, results in various sizes of a_{init}. The 2 x PDM (Planned Depot Maintenance) requirement 'check' for adjusting the test 'initiation' time does not necessarily tie in with the 0.12" a_{NDI} standard used for determining the inspectable period from crack growth calculations. It is sometimes larger or smaller [11].

The 2 x PDM time also does not account for the different growth rates of cracks under the median (50^{th} percentile) spectrum, as there is a significant concern that the rates of crack initiation and crack growth are not consistent between spectra. The LM approach uses a more consistent definition of crack initiation, a_{init}, but this value can still be very small (i.e. 0.008") and the process therefore relies on the ability of the crack growth software to predict crack growth from very small crack sizes. The a_{init} inconsistency also spoils the potential for a

[1] SICAS = Structural Integrity Assessment of Corrosion in Aircraft Structures.
[2] The material in the section is extracted from Hartley *et al.*, DSTO-TR-1856, 2005, to which the reader is directed for a detailed description of the P-3C SLAP crack initiation approach.

consistent separation between crack initiation and crack growth phases and the determination of total life as the sum of the two. The L-M processes would seem to be less rigorous than the process used by Lockheed for the interpretation of the P-3A fatigue test, where crack growth curves were used to adjust the 'test hours to initiation' to a consistent and 'readily inspectable crack size' of 0.25". It is therefore proposed that, for RAAF interpretation, a test demonstrated 'crack initiation' life be defined at a consistent crack size of 0.050". This size is essentially a compromise between the 'small crack' threshold size of, say, 0.010" and the minimum detectable crack size a_{NDI} that will be used to determine inspection intervals. Such a size is not so large that the slower crack growth in the more severe spectra will bias the setting of the time to crack initiation. The value of 0.050" is smaller than the value of 0.12" selected by Lockheed as their nominal a_{NDI}, being from an Eddy Current Surface Scan (ECSS) procedure around a filled fastener hole. However, 0.050" represents the a_{NDI} value for a Bolt Hole Eddy Current (BHEC) procedure, another common inspection procedure for the P-3C in the past, and most probably in the future. The 0.050" value will also be consistent with the a_{NDI} value used in the damage tolerance phase of the analysis.

The P-3C SLAP Program uses a crack initiation method for determining safe life [3]. This method, which is schematically depicted in Figure 1, is based on the time for cracks to grow to a detectable size (a_{init}). Figure 1 illustrates several quantities relating to the initiation and growth of fatigue cracks in the P-3C. These quantities are briefly defined in Table 1. A full description of these quantities, and their derivation, can be found in §8 of Reference [3]

The crack initiation method requires no input regarding the corrosion state of the component and assumes that NDI can detect a 0.05" (1.27 mm) crack. Fatigue crack growth models are typically only used by DSTO's P-3C SLAP team to predict fatigue crack growth beyond the detection limit. Crack growth curves were produced using FASTRAN 3.8 and the equivalent crack sizes (c_i) for coupons with and without corrosion were determined.

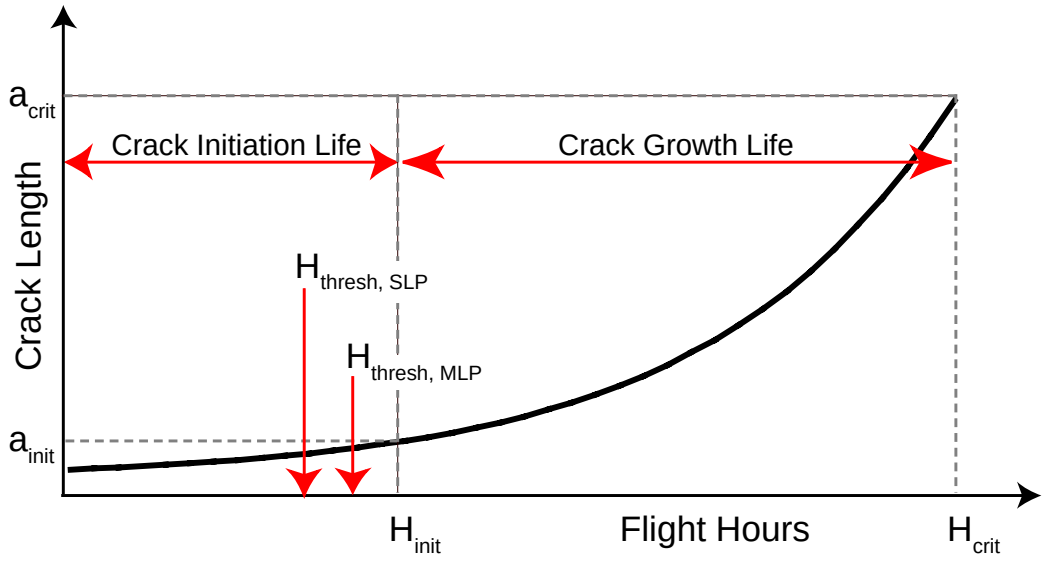

Figure 1: Method Used by P-3C SLAP: Crack Initiation (CI) where SLP is single load path and MLP multiple load path and H_{init}, H_{crit} and H_{thresh} are times of inspection intervals: initial, time at failure and time of the 1.25 mm crack initiation respectively.

Table 1: Definition of terms using in estimating the fatigue life of the P-3C

Quantity	Definition
a_{init}	Crack Initiation Length, defined as 0.05" (1.27 mm).
H_{init}	Life at which fatigue 'initiation' occurs. Note that 'fatigue crack initiation' is here defined as a crack of 0.05" length.
a_{crit}	Critical crack length at which unstable fracture occurs.
H_{crit}	Life at which unstable fracture occurs.
$H_{thresh,SLP}$	Economic life at which a crack is assumed to have initiated in single load path structure. It is defined as: $H_{thresh,SLP} = \frac{H_{crit} - H_{init}}{2}$
$H_{thresh,MLP}$	Economic life at which a crack is assumed to have initiated in multiple load path structure. It is defined as: $H_{thresh,MLP} = \frac{Total\ Life}{3} = \frac{H_{crit}}{3}$
H_{NDI}	Life at which non-destructive inspection becomes necessary to ensure continued airframe structural integrity. Defined as equal to H_{init}.
Initiation Life	Life from the start of airframe service until the initiation of the first detectable crack of 0.05" length.
Growth Life	Life from the initiation of a detectable fatigue crack until fast fracture.
Inspection Interval	Interval, in flight hours, at which NDI inspections should be commenced. It is defined as: $H_{NDI} = \frac{H_{crit} - H_{NDI}}{2}$

3.2 The Equivalent Crack Size (ECS) approach

3.2.1 Fundamental ECS Method

The ECS approach is a potential method by which pitting corrosion can be treated as a fatigue crack, assuming it is no longer growing due to corrosion. The ECS concept is a modification of the EIFS concept which was originally suggested by Rudd and Gray [12] as a means of estimating the effect of initial surface state on fatigue life. If successful in predicting the effects of corrosion, the ECS approach could allow corrosion pits to be evaluated using the same criteria used for fatigue cracks. Maintenance actions could then be scheduled more economically than using the 'find and fix' policy. If it could be shown that pitting corrosion was not going to cause an unacceptable loss of structural integrity prior to the next depot maintenance then the removal of the corrosion could be delayed to that time. This would reduce maintenance costs and increase aircraft availability.

The underlying assumption of the ECS approach is that a pit of a certain size will act like a crack of a related size [12-19]. Given accurate fatigue crack growth (FCG) data, the fatigue crack initiated from the pit will grow in an identical manner and at the same rate as that from

the 'equivalent crack' after an initial stage during which the fatigue crack from the pit is established. This is illustrated in Figure 2. Once the relationship between pit size and equivalent crack size has been established it should be possible to treat pits as if they were cracks. However, determining the relationship between pit size and crack size requires extensive laboratory testing. One such program at DSTO utilised over 400 fatigue life tests [11] to provide statistical confidence and investigate the effect of load ratio.

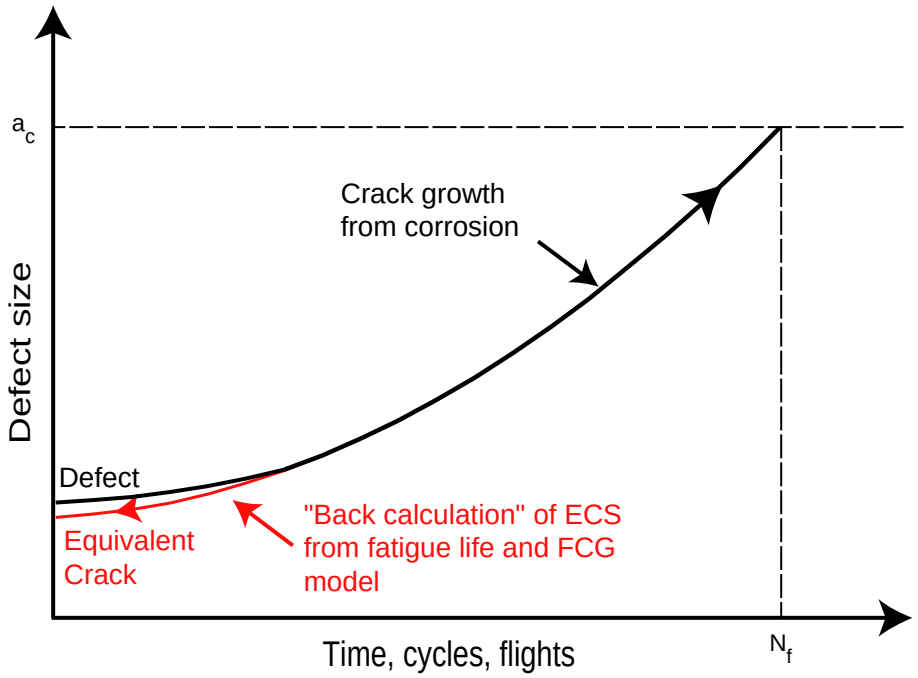

Figure 2: Relationship between ECS and Defect (Pit) Size and the similarity of crack growth from each

In addition, the definition of pit size apparently varies with material. Previous DSTO work [20] has shown that pit depth is a good metric for D6ac steel, while in 7050, (pit depth * pit aspect ratio) is the most effective metric [21]. In contrast, for 7010-T7651, pit cross-sectional area was the most effective metric [11]. One of the principal parts of developing an ECS, therefore, is identifying a suitable metric for pit size. Figure 3 illustrates the parameters that can be used to characterise a pit's size. These include:

- Pit cross-sectional area
- Maximum pit depth
- Maximum pit width
- Pit surface opening width
- Local pit radius
- Pit aspect ratio = ½(maximum pit width)/(maximum pit depth)

It should be noted, however, that some of the above quantities cannot be measured in-service. More likely metrics for in-service use include maximum pit depth, maximum pit width and pit opening width. As can be seen in Figure 3 the maximum depth of a pit can exceed its apparent depth due to the complex shape of the pit. Corrosion pits in aluminium alloys tend to be very convoluted in shape making it very difficult to examine them in-service.

Furthermore, corrosion pits in aluminium alloys are commonly full of corrosion product. In the current work limitations imposed by NDI were deliberately ignored as the aim was to assess the effect of corrosion on the safe life methodology used on the P-3C, not to provide a management plan for the detection and assessment of corrosion.

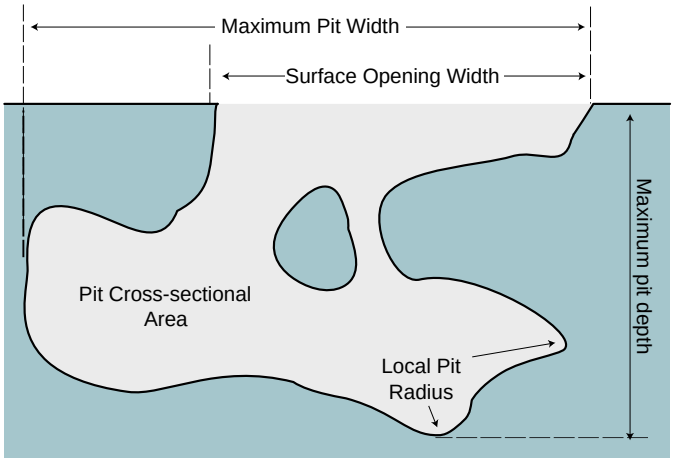

Figure 3: Various measures of pit size for use as pit metrics

3.2.2 Crack Metric Ratio (CMR) Extension of the ECS Method.

In the SICAS project, which investigated the effect of pitting corrosion on the fatigue life of 7010-T7651, the ratio between the crack size input into AFGROW [22, 23], a fatigue crack growth estimation code, and the measured pit metric was used to control the estimation of the ECS[3]. This ratio was termed the 'Crack Metric Ratio' and was defined as:

$$CMR = \frac{ECS}{Pit\ Metric}$$

Examination of the distribution of CMR values for the entire fatigue life dataset obtained in the SICAS project showed that they were log-normally distributed. Therefore, the distribution of CMR values could be described by two terms; the log mean CMR value, $CMR_{logmean}$, and the log-standard deviation value, CMR_{logSD}.

The log-normal nature of the CMR values was useful as the magnitude of the pit metric was observed to have a statistically significant but weak effect on fatigue life. The log-normally distributed nature of the CMR values meant that 'safe ECS' values could be readily estimated. This allowed any arbitrary level of safety, defined here as probability of failure, to be applied to the calculation of the fatigue life of pitted 7010-T7651. In the case of the SICAS project, a 1 in a 1000 safety level was used. To calculate this, the equation above needs to be rewritten as:

$$ECS\ Area = CMR \times Pit\ Metric$$

[3] In the SICAS project, the term Equivalent Initial Flaw Size (EIFS) was used instead of the current term ECS.

If logarithms are taken of both sides of this equation it becomes:

$$\log(ECS\ Area) = \log(CMR) + \log(Pit\ Metric)$$

If $CMR_{logmean}$ is used in this equation then the prediction of fatigue life made will be equally distributed either side of the actual fatigue life [2]. This gives:

$$\log(ECS\ Area) = \log(CMR_{\log mean}) + \log(Pit\ Metric)$$

or

$$ECS\ Area = CMR_{\log mean} \times Pit\ Metric$$

For a normal distribution the mean plus three standard deviations is approximately equal to a cumulative probability of 0.999. Therefore if the CMR value given by:

$$CMR_{p\approx 0.999} = CMR_{\log mean} \times \left(CMR_{\log SD}\right)^3$$

is used in estimating fatigue life then approximately 99.9% of the fatigue life estimates will be conservative. An example, from the SICAS project, of using a CMR modified in this manner is shown in Crawford et al. [2], see Figure 4.

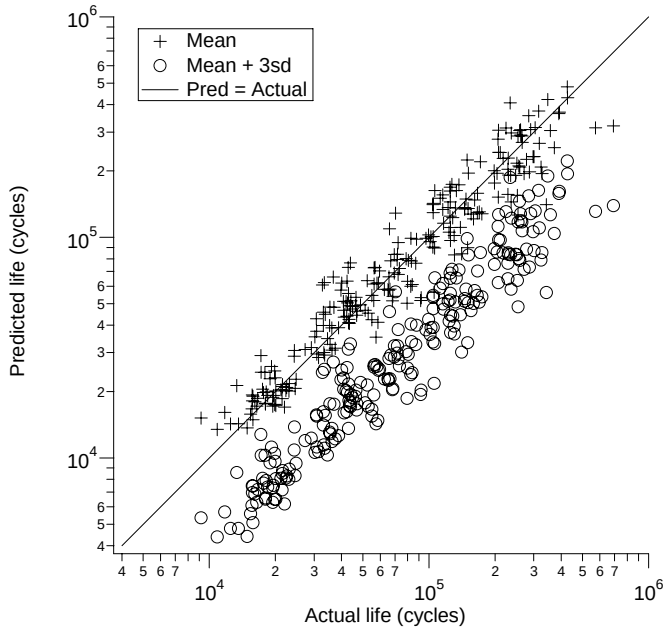

Figure 4: Effect of using mean and mean+3SD values of crack metric ratio on the prediction of fatigue life for 7010-T7651 tested under constant amplitude conditions. Data derived from the SICAS project [1, 2].

4. Experimental Material and Method

The experimental programme consisted of three parts. These were:

1. Establishing a corrosion protocol and corroding fatigue specimens according to it;
2. Fatigue testing and fractography of un-corroded (control) and corroded specimens; and
3. Crack growth modelling and formulation of ECS distribution and CI estimates.

Each part of the experimental programme and the experimental material used are discussed below in separate sections.

4.1 Experimental Material

The material used in this experimental programme was 3 mm thick AA 7075-T6 sheet clad with an approximately 100 μm thick Alclad layer on each face. This material was the same as that used in the P-3C Test Interpretation report [3]. It is worth noting that the 7075-T6 used on the P-3C is typically unclad extruded material. However, material availability issues and continuity with previous work [3] required the use of Alclad material.

4.2 Corrosion of Specimens

Blanks of the experimental material of 10 x 10 mm (100 mm^2) were set in epoxy. These blanks were in as-received condition. The surface of the blanks was charged by aerosol application of 3.5 wt% NaCl solution to provide coverage of 5 mg/cm^2 NaCl. All exposures were at 90% relative humidity and up to three cycles of both 24 and 48 hours were trialled. Six conditions were examined: 1, 2, or 3 applications of either 24 hr or 48 hr exposures. The blanks were dried between each cycle for 4 hours at 45°C. All trials were conducted using an environmental chamber.

Pit depth measurements were taken by serial sectioning using an ultra-mill with high-resolution digital imaging to determine the number of incremental 5 μm cuts required to completely remove the corrosion in a given area. Five blanks were used for each condition and the data obtained were analysed to predict the expected pit depths in the fatigue critical region of the fatigue specimens.

The first step in the analysis was the collection of data to determine the distribution of pit sizes. The fatigue critical regions of the specimen were extremely small, and targeting corrosion in these areas was a challenge. The pitting data collected here were modelled using extreme value statistics [24-27]. These were appropriate for several reasons. Typically, pitting corrosion damage is evaluated using average pit depth measurements, which can be easily extrapolated using growth laws to longer exposure periods. This standard method, however, provides no information regarding the largest pits that control fatigue endurance.

Extreme value statistics have been used here as in other pitting studies due to their ease of measurement and the quality of the output from these models. For these reasons, they are

widely used in the water supply industries [28] where leaks due to pitting are a very significant cost and in the nuclear power industry where leakage poses a grave risk [26].Without extreme value statistics, it would be necessary to measure the size of every pit on the surface of the sample or to measure the largest pit on a very large number of samples. This is impractical and also very difficult at the lower end of the size scale where pit depths are small and pit numbers high.

The data were analysed using extreme value statistics by ranking the largest pit in each of the blanks in order of increasing size. The probability of a random selection being less than or equal to the ranked value is given by:

$$\Pr_i(X \le x) = \frac{i}{n+1},$$

where n is the number of observations and i is the *ith* observation ranked in order of increasing size[4]. The theoretical probability can then be expressed in terms of a cumulative distribution function as:

$$\Pr(X \le x) = (F(x))^n$$

where n is the number of observations or sections examined.

$F(x)$ is typically derived from a family of distributions. For three classic distributions (commonly termed Type I, Type II and Type III) [24],

$$(F(x))^n = F(a_n + b_n x)$$

Type I distributions include normal, exponential and Weibull distributions and are unlimited distributions. That is, there are no upper or lower bounds to the value of x in these distributions. This means that $F(x)$ is greater than zero for all real values of x. Type II and III are limited distribution in that Type II distributions have upper bounds and Type III distributions have lower bounds. A Type I, exponential distribution of the form:

$$F(x) = 1 - \exp([-\frac{(x-\mu)}{\alpha}])$$

was used in this work. It is common practice to use Type I distributions in modelling maximum pit size distributions due to their mathematical simplicity compared to Type II and III distributions.

The corrosion protocol selected was three cycles of 48 hours of exposure at 90% relative humidity and 5 mg/cm^2 NaCl with drying periods between each cycle. The multiple cycles increased the number of pits per unit area and were needed to increase the probability of a

[4] Note that this function is arbitrary but is commonly used as it avoids the problems associated with probabilities of 0 and 1 at $i = 1$ and $i = n$, respectively.

significant pit in the extremely small fatigue-critical area, approximately 1 mm², on each fatigue specimen. The predicted distribution of maximum pit sizes in the corroded specimens that were to be subject to fatigue is shown in Figure 5 along with the largest pit found on each of the 18 specimens which failed due to corrosion as cumulative probabilities. The offset is probably a result of the assumed area on the test coupons that is fatigue critical. This was assumed to be 2 mm^2 while the actual value is unknown.

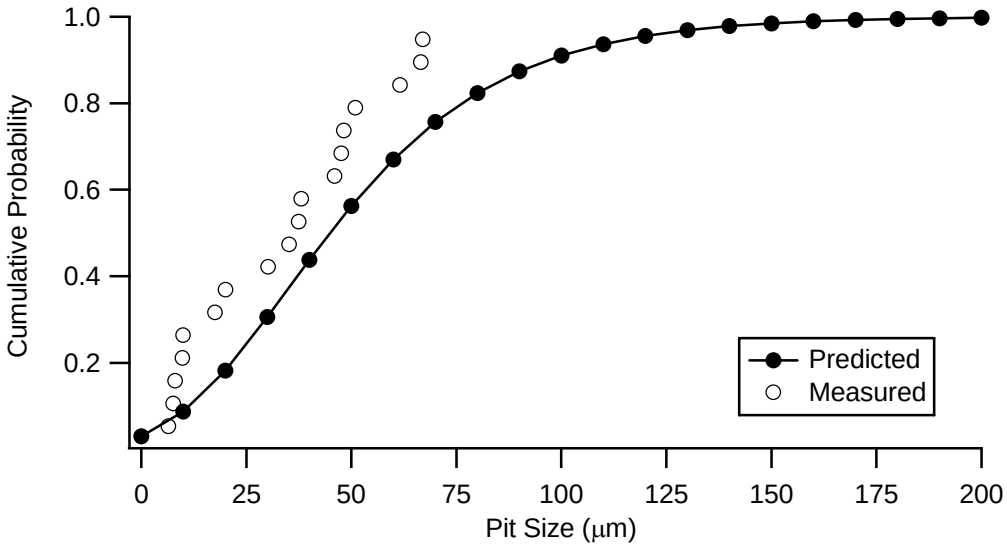

Figure 5: Comparison of predicted pit depths and measured pit depths

4.3 Fatigue and Fractography

Fatigue testing was carried out using a flight spectrum designed by DSTO's P-3C SLAP team to represent Australian usage conditions. This spectrum, which is plotted in normalised form in Figure 6, is a variable amplitude tension dominated spectrum containing about 1.6 million turning points. The spectrum was clipped on the negative side at -20 ksi and all loads of less than 2 ksi magnitude were truncated.

Testing was carried out in accordance with ASTM E739 [29] for metallic materials at two load levels, 15 and 17 kN, representing peak stresses of 124 and 140 MPa. A total of 22 un-corroded and 22 corroded specimens were tested (see Table 2). The specimen geometry, which contains a hole with a stress concentration factor (Kt) of 5, is shown in Figure 7. The specimens were of a high-Kt geometry intended to mimic the stress state in and around holes in the P-3C airframe. These specimens were originally developed for the fatigue coupon testing program that was conducted in support of the P-3C SLAP program [30].

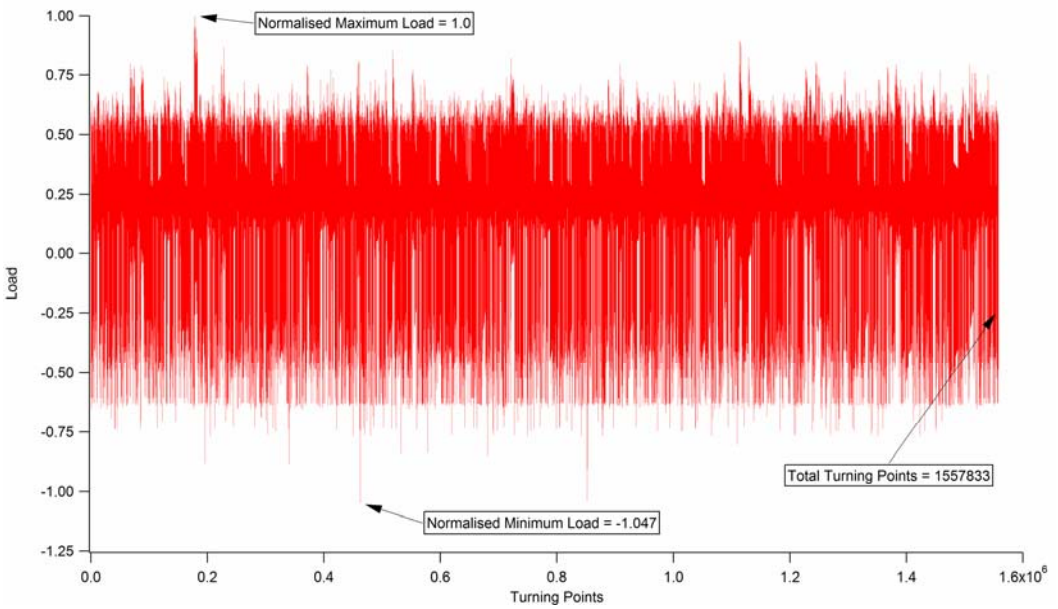

Figure 6: RAAF P-3C Fatigue Critical Area 361R spectrum normalised with respect to maximum tensile load

Post-failure fractographic examinations were performed using a LEO Scanning Electron microscope using secondary electron imaging. Pit cross-sectional area, width and depth were recorded for pits exhibiting significant fatigue. The dominant initiator was assumed to be that from which the largest fatigue crack had grown. Only two cases were noted with multiple initiators within close proximity and these were removed from the study.

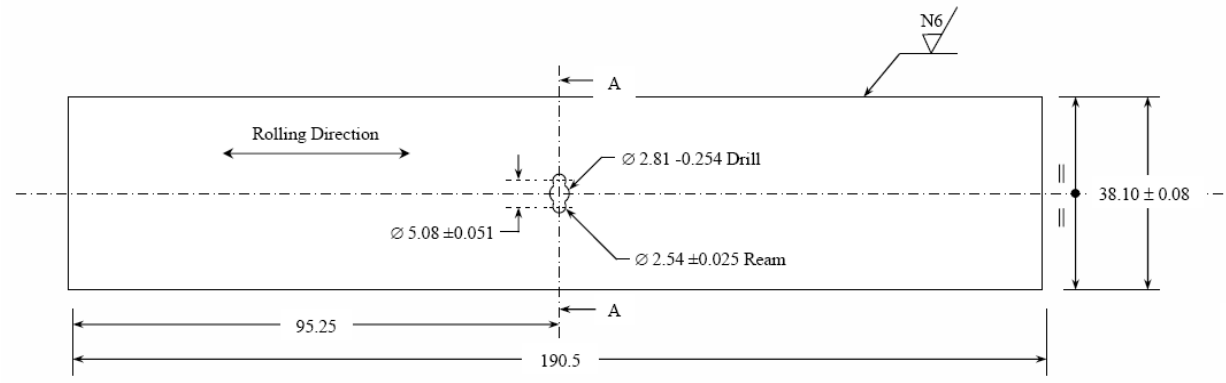

Figure 7: Geometry of Kt = 5.0 fatigue specimen [30]. Dimensions are in mm

Table 2: Experimental Matrix

Peak Load (kN)	Peak Stress (MPa)	Specimen Quantity	
		Corroded	Un-corroded
15	124	11	11
17	140	11	11

4.4 Crack Growth Modelling

Previous DSTO research on how corrosion affects fatigue life was conducted using AFGROW. In the current work, however, FASTRAN [31] was used as it is the fatigue prediction code used by the P-3C SLAP. FASTRAN is a computer model that predicts the propagation of fatigue cracks under constant and variable amplitude loading. It was originally developed by James C. Newman Jr. when he worked at NASA's Langley Research Centre. Dr. Newman subsequently left NASA and now works at Mississippi State University where he has continued to develop FASTRAN. It is currently up to Version 5.0, which is a commercial product. FASTRAN Version 3.8 is the last publicly available version. Much of the published research relating to FASTRAN was performed using FASTRAN II [31].

The fatigue crack growth analysis was performed using FASTRAN 3.8 with geometry factors derived from finite element analysis. The average[5] final crack length and the average crack growth life from the fatigue tests were used as a target for the modelling and the model's results were matched to the target lives by changing the initial crack size. That is, if the model underestimated fatigue life then a smaller initial crack size was used. Conversely, if the model overestimated fatigue life then the initial crack size was increased.

5. Results and Discussion

5.1 Fatigue Results

The fatigue life results obtained for the 15 kN and 17 kN peak loads are shown in Figure 8[6]. The reduction in fatigue life due to corrosion is apparent. Corrosion reduced the median fatigue life by 17% at 15 kN and caused a 27% reduction in median life at 17 kN. Furthermore, the fatigue life results for the corroded and uncorroded specimens do not overlap in either the 15 kN or 17 kN load cases. The significance of this reduction in terms of the safe life of the component cannot be directly assessed as it would require the corrosion to be representative of in-service corrosion and would only be appropriate for the specific specimen geometry and load.

[5] In this context average is the average crack length for all specimens tested at a given load (i.e. 15 or 17 kN).
[6] See Appendix A for a complete fatigue life data set.

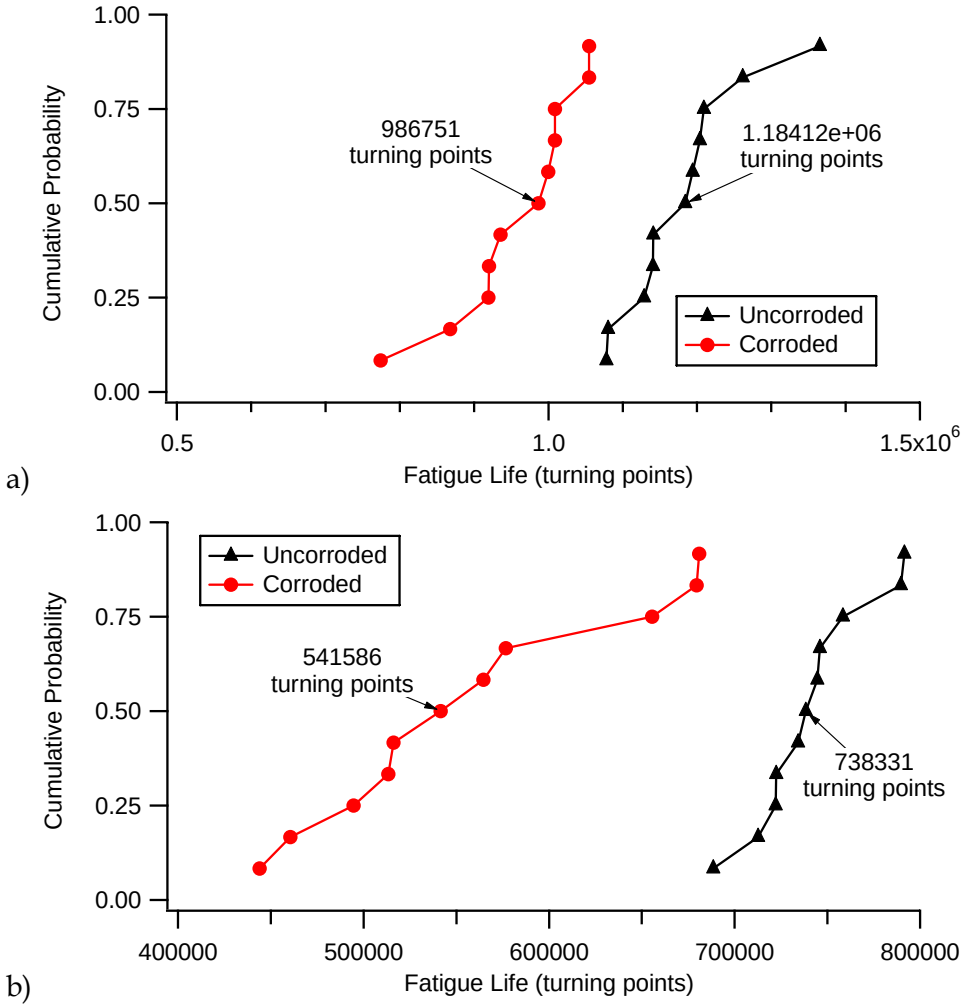

Figure 8: Effect of corrosion on fatigue life for (a) 15 kN and (b) 17 kN peak stress levels. Median fatigue lives for each corroded and uncorroded conditions are indicated.

5.2 Fractography

Fatigue initiation mechanisms were identified by fractographic examination of the corroded and un-corroded specimens in a scanning electron microscope (refer §4.3). Crack initiation occurred either at the corners of the stress concentrating hole or from corrosion pits. Corner failures occurred due to cracks initiated either within the softer Alclad material from machining defects, such as burring, at the corners of the specimens or through preferential corrosion of the Alclad layer. It is important to note that although the corrosion of the Alclad layer was many times larger than individual pits, typically encompassing the entire thickness of the Alclad layer, fatigue initiation via this mechanism was rare. Figure 9(a) shows an observed corner crack corrosion failure from the Alclad layer. A failure from a pit is shown in Figure 9(b) with river marks radiating from the corrosion pit. Figure 10 shows the mechanisms observed for the failure on the un-corroded specimens. Figure 10(a) shows a failure resulting from burring on the edge of the hole. Figure 10(b) shows the thickness of the Alclad layer and another example of burring.

a)

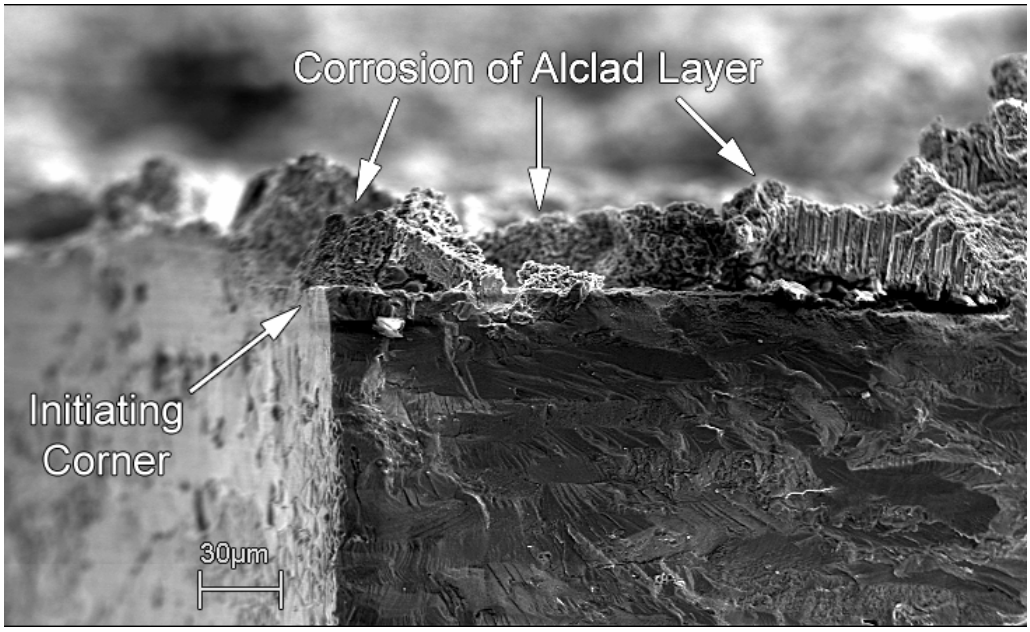

b)

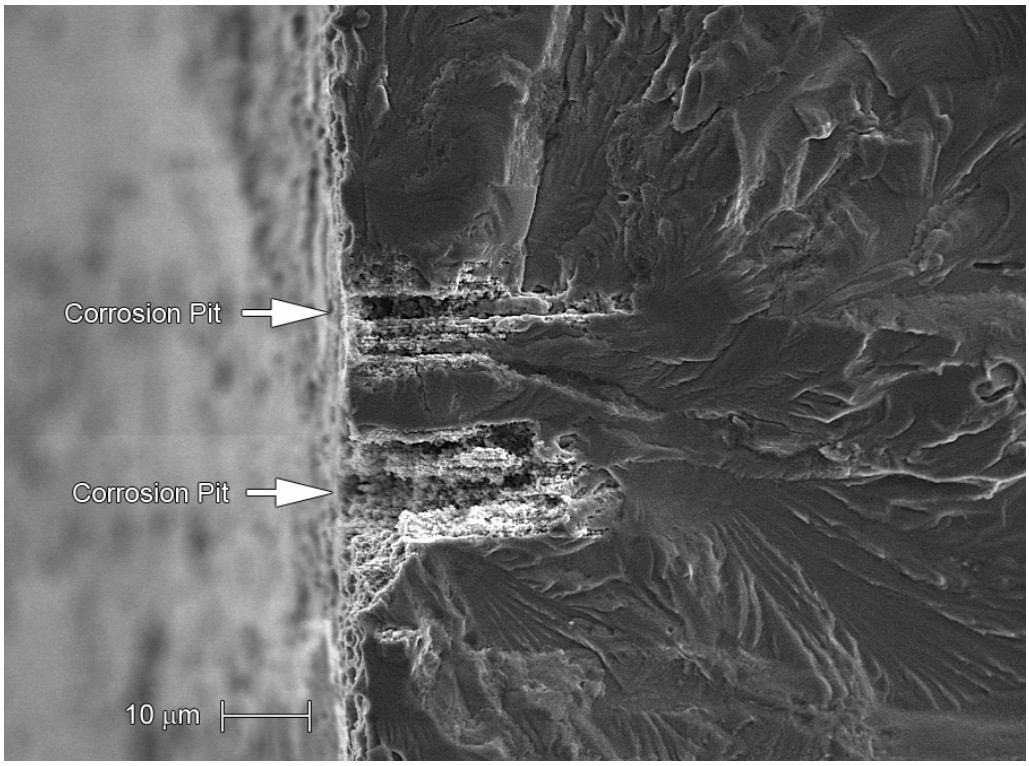

Figure 9: Initiation sites associated with corrosion; (a) corner-initiated failure and (b) pit-initiated failure. Initiation sites are indicated by arrows.

a)

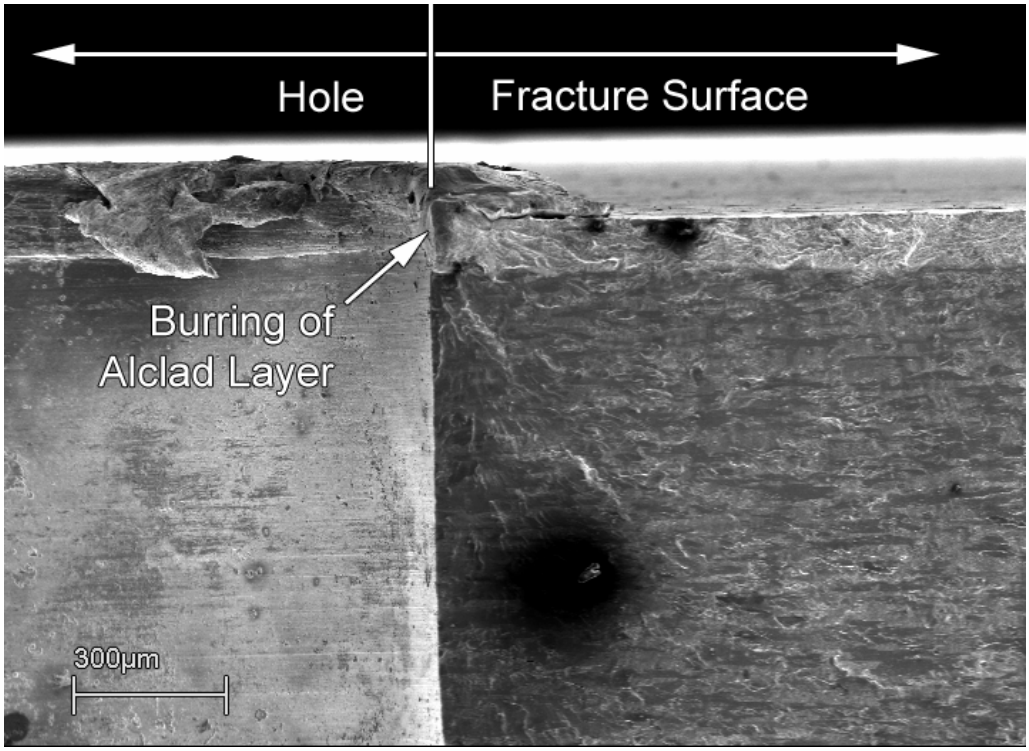

b)

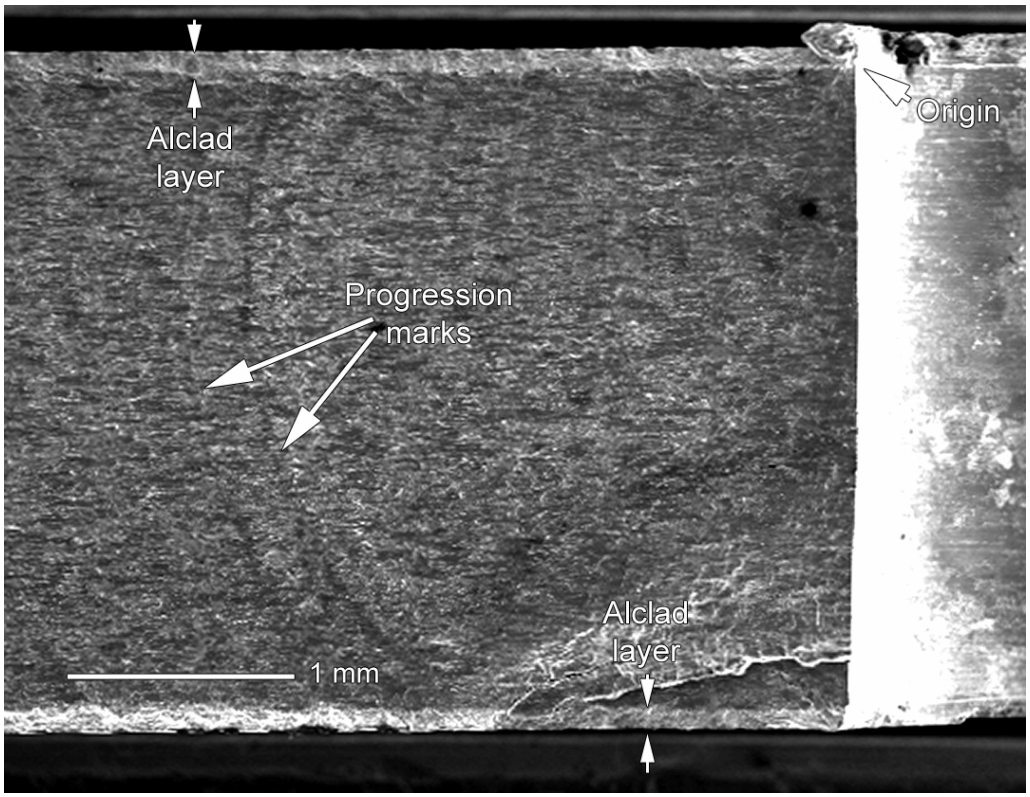

Figure 10: Initiation sites unrelated to corrosion; (a) Lapping/Burring and (b) Alclad layer and burring

5.3 Pit Metric Results

Following fatigue testing, all of the corroded specimens were cleaned using concentrated nitric acid (HNO_3) for two minutes in an ultrasonic cleaner. This is a modification of a method for removing corrosion product from aluminium alloys detailed in ASTM G-1 [32] as using the ultrasonic bath enhances the cleaning of the corrosion pits. Previous work on the SICAS project showed that this method does not damage fracture surfaces [1].

Measurements were made of the primary initiating pit on each coupon, post fracture, from SEM images. The measurements made were maximum pit depth, width and area. From these values, suitable metrics for characterising the severity of an individual pit were determined.

The results were examined to determine if the initiating pit size varied with the stress levels used. This could occur as a result of statistical anomalies or due to a change in the fatigue initiation mechanism (e.g. a shift to corner cracks). Table 3 and Table 4 show the results of this analysis. Examination of Table 3 might suggest that pit depth and pit area metrics varied with load level. However, the more rigorous analysis in Table 4 shows that there was no statistically-significant effect of load level on pit metric. This is indicated by the low value of *t* and the 95% confidence interval including zero for all metrics. Thus, although the means appear different, it is impossible to determine if the samples came from different populations. It is therefore acceptable to pool the data from both load levels into a single data set.

Table 3: Descriptive statistics for measured pit metric by stress level

Pit Metric	Stress	N	Mean	Standard Deviation	Standard Error Mean
Depth	15.00	8	30.6	24.8	8.77
	17.00	10	35.0	18.5	5.85
Width	15.00	8	39.4	13.5	4.76
	17.00	10	38.1	16.0	5.06
Area	15.00	8	617	606	214
	17.00	10	840	912	288

Table 4: T-test for determining difference of means for Pit metrics by stress level

Pit Metric	t	Degrees of Freedom	Sig. (2-tailed)	Mean Difference	Std. Error Difference	95% Confidence Interval of the Difference	
						Upper	Lower
Depth	-0.436	16	0.669	-4.44	10.2	-26.0	17.2
Width	0.192	15.934	0.850	1.33	6.94	-13.4	16.1
Area	-0.622	15.577	0.543	-223	359	-987	540

6. Analysis

6.1 Identification of Statistically Significant Pit Metrics

Given the results in §5.3, which show no relation between pit metrics and loading, a multiple linear regression using all the pit metric data was performed to identify which pit metrics were statistically significant with respect to fatigue life. The independent parameters input into the model were pit width, pit depth, pit area and applied stress. Tests were undertaken as part of the modelling process to iteratively remove the least statistically significant of the independent parameters. The model produced the results shown in Table 5, which show that pit area was the only significant pit metric. Pit width and depth were removed as being insignificant in the first and second iterations, respectively, of the model. Note that in the final results (Iteration 3), a parameter was considered significant if the absolute value of its t-statistic was greater than 2 [1, 2, 33]. As can been seen in Table 5, pit area has a t-statistic above this value. However, the t-statistic of the applied stress is far higher, indicating that stress has a greater effect on fatigue life than the size of the initiating pit. Similar results were observed in the SICAS project [1].

Table 5: Linear Regression Model for Measured Pit Metrics and Stress versus Life. Shaded rows indicate least significant parameter for removal in subsequent iterations.

Iteration	Parameter	Unstandardized Coefficients		Standardized Coefficients	t	Significance
		B	Std. Error	Beta		
1	(Constant)	3909824	281848	—	13.872	0.000
	Depth	1705	2304	0.162	0.740	0.472
	Width	1516	2214	0.100	0.685	0.505
	Stress	-194191	16802	-0.902	-11.557	0.000
	Area	-6810	5286	-0.359	-1.288	0.220
2	(Constant)	4008661	237489	—	16.879	0.000
	Depth	458	1386	0.044	0.331	0.746
	Stress	-198984	14983	-0.924	-13.280	0.000
	Area	-3650	2532	-0.192	-1.441	0.171
3	(Constant)	4013581	229878	—	17.460	0.000
	Stress	-199449	14468	-0.926	-13.785	0.000
	Area	-2934	1274	-0.155	-2.302	0.036

Given that the crack growth model was one dimensional and therefore required lineal inputs (i.e. crack width and depth are lineal not areal dimensions), pit area was converted to a lineal dimension by taking the square root. In doing so, the method assumes that the aspect ratio of the modelled pits is the same in all cases, but does not assume a value, as a shape factor here will carry through to the crack metric ratio. The next test was to prove that ECS was not stress dependant, and thus, results from different stress levels could be pooled rather than being treated as individual cases.

6.2 Calculation of Equivalent Crack Sizes

Equivalent crack sizes for each specimen that failed from corrosion were determined using a master curve of initial crack size vs. fatigue life derived using FASTRAN. This model used a range of input crack sizes that produced a range of fatigue lives bracketing those observed in testing. ECS values were then determined by interpolation. Figure 11 shows the relationship between the FASTRAN derived ECS value and fatigue life (in turning points). As expected, fatigue life decreases with an increase in either applied stress or initial crack size.

The ECS data shown in Figure 11 were analysed statistically to determine if there was any dependence of ECS on applied stress. Table 6 and Table 7 show the results of this analysis. As expected from Figure 11 the data from the tests conducted at a load of 17 kN have a larger standard deviation. However, the analysis of variance of these data in Table 7 shows that there was no significant difference between the 15 kN and 17 kN data. Therefore, the ECS results from each applied load were pooled into a single data set. The mean ECS value of this dataset is 35.5 μm.

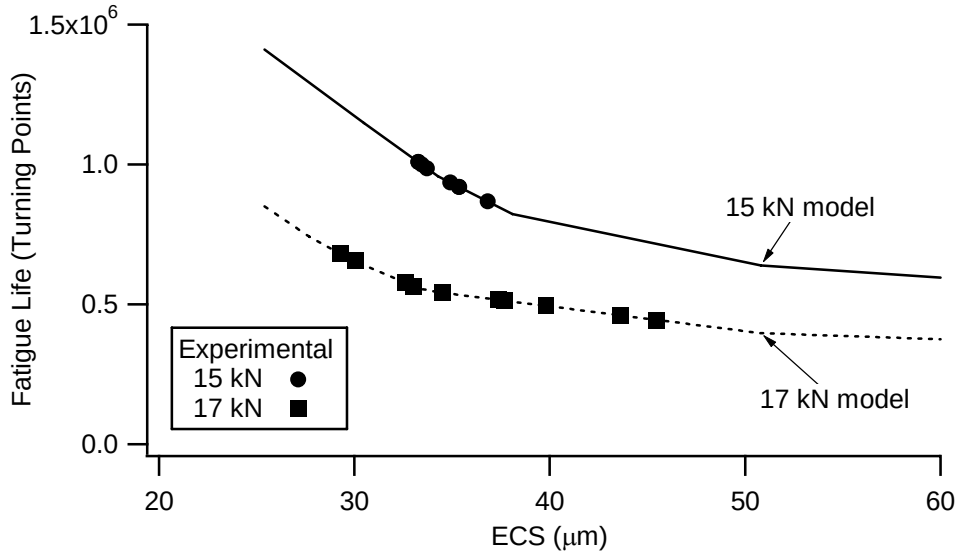

Figure 11: Relationship between ECS value calculated using FASTRAN and fatigue life in turning points as a function of applied load. Data points indicate the corresponding ECS for each sample that failed due to corrosion.

Table 6: ECS descriptive statistics by stress level

Load (kN)	N	Mean (μm)	Std. Deviation (μm)	Std. Error Mean
15	8	34.5	1.30	0.459
17	10	36.3	5.46	1.73

Table 7: T-test for difference of means between 15 kN and 17 kN data

Variance	t	Degrees of freedom	Sig. (2 tailed)	Mean Difference	Std. Error Difference	95% Confidence Interval of the Difference	
						Lower	Upper
Equal	-0.919	16	0.372	-1.8242	1.98552	-6.03329	2.38494
Unequal	-1.021	10.249	0.331	-1.8242	1.78729	-5.79344	2.14509

6.3 Calculation of Crack Metric Ratios

The relationship between CMR and the linear pit area metric for the current case is shown in Figure 12. A similar method was used by Crawford et al. [13]. In the previous study, CMR was observed to be a constant ratio for pits with linear dimensions above approximately 100 μm. ECS is an empirical methodology and has no mechanistic basis for its predictions. As such, ECS cannot be used to extrapolate outside of the boundaries of tested conditions. In the previous study, corrosion of sizes under 100 μm were not investigated and the behaviour shown in Figure 12 was not apparent. This behaviour indicates that either:

1. An additional mechanism is active with pit sizes below 100 μm. An example would be a process zone around the pit that is small in comparison to pits larger than 100 μm but becomes important at lower pit sizes, or
2. The crack growth modelling at lower pit sizes (and ΔK values) is inaccurate.

It is quite possible that the variation of CMR below 100 μm is due to small/short crack growth behaviour, such as first reported by Pearson [34].

A 'safe' CMR relationship was established by performing an error analysis between the data points and the modelled relationship. The error was determined to follow a normal distribution using a one sample Kolmogorov-Smirnov test [33]. A safe curve was then determined by shifting data points by three standard deviations, creating a CMR that would only be reached by approximately one in one thousand pits. This relationship allows a safe ECS to be determined for a given pit metric (Figure 12).

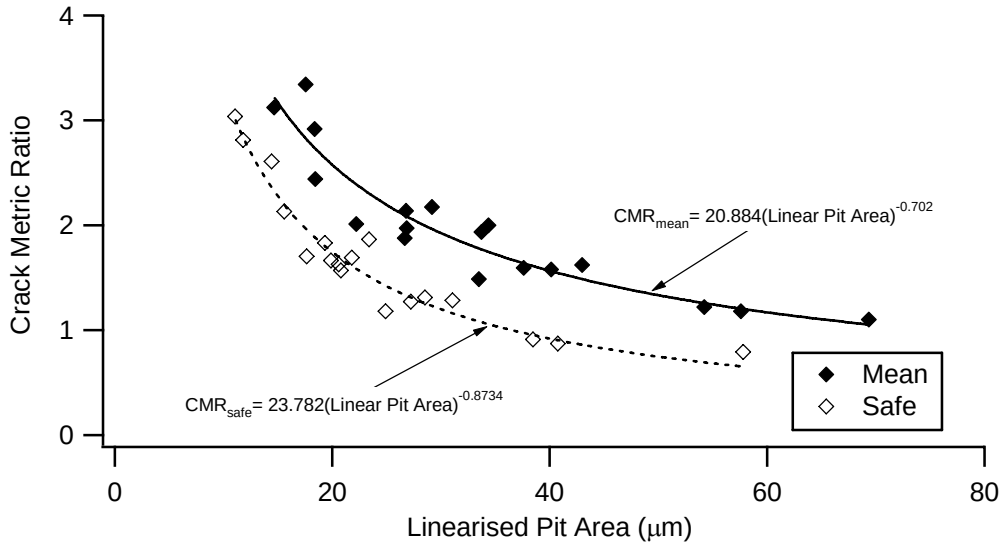

Figure 12: Relationship between crack metric ratio and pit metric for mean and safe (p = 0.001) CMR

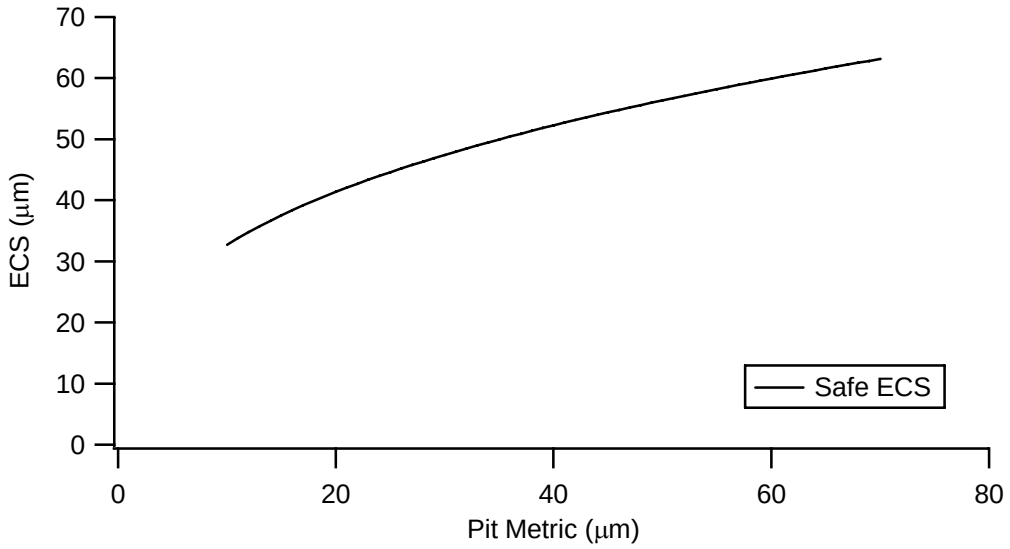

Figure 13: Relationship between pit metric and Safe Equivalent Crack Size

This safe ECS can then be transformed into corresponding 'safe' fatigue lives at any stress level for any severity of corrosion within the bounds of the corrosion and stress levels tested here, Figure 13. These are shown in Figure 18 along with the comparison with the safe lives determined through crack initiation methods for single and multiple load path structure calculated in §6.4

6.4 Calculation of Time to Crack Initiation

Crack growth curves were produced using FASTRAN 3.8 and the equivalent initial crack sizes (c_i) for coupons with and without corrosion were calculated. This was done by iteratively inputting different values of c_i into the model until a close match to the observed average test life was achieved. The results of this modelling are presented in Table 8.

Table 8: Equivalent crack sizes for coupons with and without corrosion

Load (kN)	Stress (MPa)	Corroded	Average a_{crit} (mm)	Average Test life (turning points)	c_i, (mm)	c_i - c_{notch} (mm)	Increase due to corrosion (mm)
15	124	No	15.9	1180653	2.824	0.03	–
15	124	Yes	15.9	957322	2.828	0.034	0.004
17	140	No	15.9	740740	2.823	0.029	–
17	140	Yes	15.9	557042	2.827	0.033	0.004

Note that average a_{crit} denotes the average of the final crack sizes calculated using the FASTRAN model and c_{notch} was equal to 2.794 mm (0.11"). The increase due to corrosion is the difference between the c_i for the corroded and uncorroded states at each load level.

As FASTRAN3.8 does not have an exact crack type for this specimen, the user defined crack type was used (NTYP=-99). This crack type only allows the simulation of through cracks, as it is a one-dimensional model. The crack growth behaviour is defined by the user supplied geometry factors (β-factors).

The β solution from a DSTO 3D FE analysis was used. The original β factors were defined against the crack length measured from the notch root, but in FASTRAN it should be measured from the centre of the specimen. Therefore the crack lengths and β-factors needed to be converted, while keeping the corresponding stress intensity factor identical, i.e.

$$K = \beta_n S\sqrt{\pi c_n} = \beta_c S\sqrt{\pi c_c}$$

Where c_n and c_c are the crack lengths measured from the notch and the centre, respectively, and β_n and β_c are the corresponding β-factors. From the above, the β-factors used in FASTRAN are given by:

$$\beta_c = \beta_n\sqrt{\frac{c_n}{c_c}} = \beta_n\sqrt{\frac{c_n}{R + c_c}}$$

where R is the notch root radius.

'c_i' denotes the initial crack size calculated to match the final crack sizes and fatigue lives measured experimentally and was used only to provide a starting point for the production of the crack growth curves given in Figure 15. The crack initiation method is used in the SLAP program because confidence in the validity of the crack growth curves is only achieved for crack sizes greater than 1.25mm [11] .

The finite element analysis the β-factors are based on uses the central line of the specimen as its starting point, therefore, the surface of the crack is at a distance of 0.055". The value of a_{init} was therefore set at 0.105" corresponding to 0.05" of crack growth. Threshold values for safe-lives for single and multiple load path structure were then determined from the crack growth curves plotted in Figure 14 and Figure 15 and are summarised in Table 9. For both load cases, corrosion reduced the time to crack initiation by approximately 26%. Figure 16 plots the predicted crack growth curves for 17 kN load for the corroded and uncorroded cases. The corroded trace has been offset by the difference in H_{init} (Table 9) to illustrate how crack propagation after crack initiation is unaffected by corrosion. It should be noted, however, that this is a result obtained from modelling and requires experimental validation.

Table 9: Times of inspection intervals: initial, time at failure and time of the 1.25 mm crack initiation

Load (kN)	Stress (MPa)	Corroded	H_{crit}	H_{init}	$H_{thresh,\ SLP}$	$H_{thresh,\ MLP}$	ΔH_{init}
15	124	No	1180653	973600	103526	393551	–
		Yes	957322	723000	–	–	-26%
17	140	No	740740	559300	90733	246913	–
		Yes	557042	413300	–	–	-26%

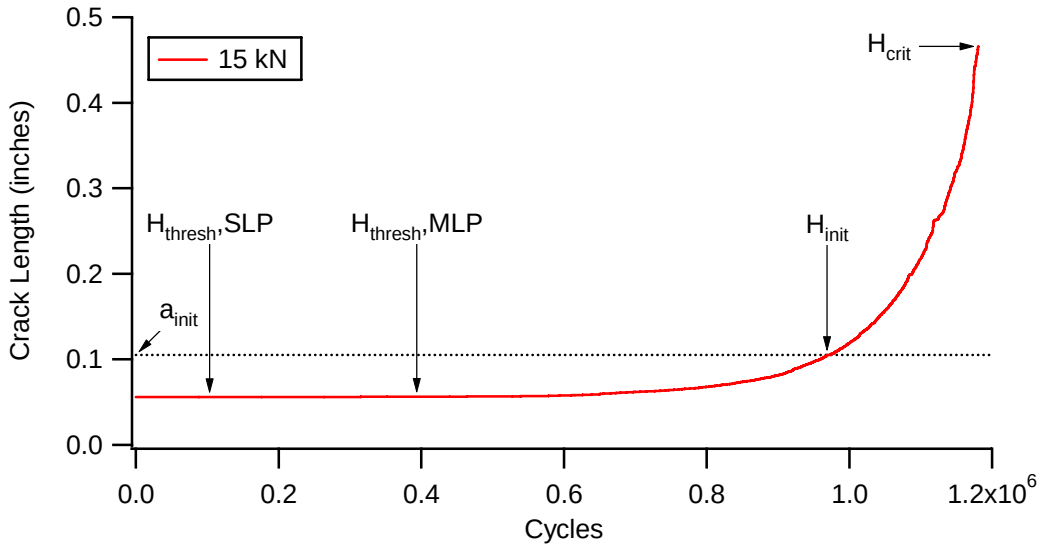

Figure 14: Crack Initiation (CI) for uncorroded specimens where SLP is single load path and MLP multiple load path and H_{init}, H_{crit} and H_{thresh} are defined in Table 1. Applied maximum load was 15 kN.

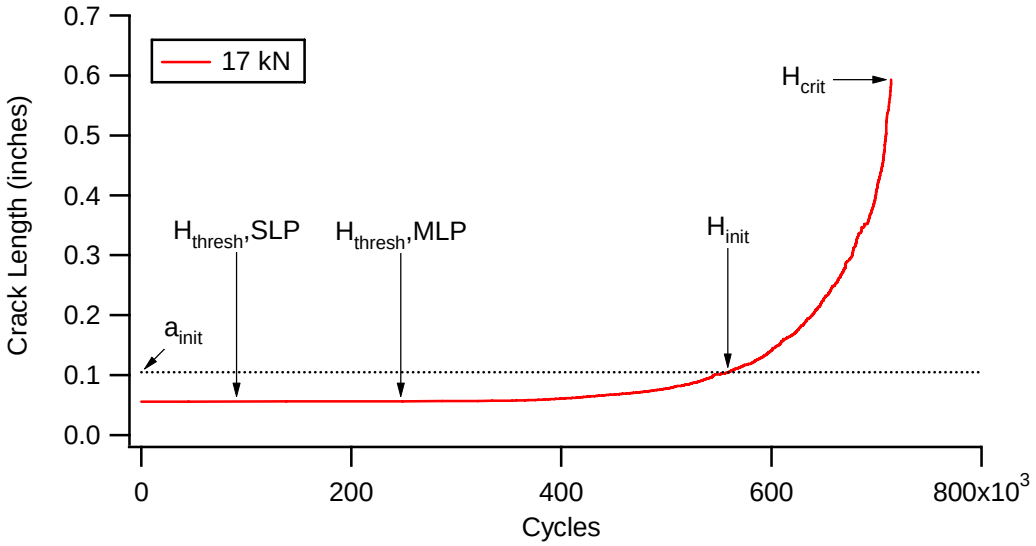

Figure 15: Crack Initiation (CI) for corroded specimens where SLP is single load path and MLP multiple load path and H_{init}, H_{crit} and H_{thresh} are defined in Table 1. Applied maximum load was 17 kN.

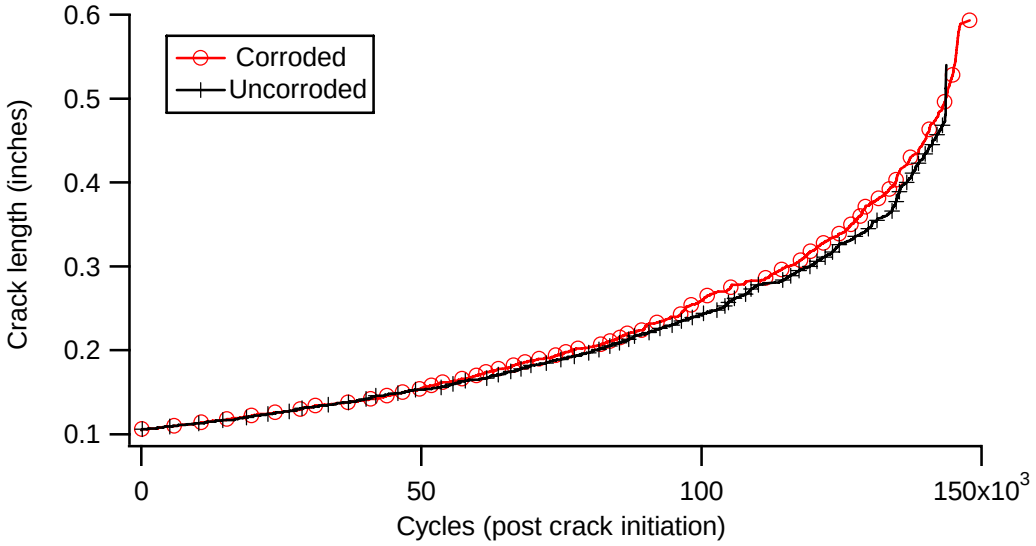

Figure 16: Comparison of crack growth traces

By comparing the threshold values of the safe-lives for single and multiple load path structure to the fatigue results for the corroded specimens, it is apparent that the corroded lives exceed the threshold values, Figure 17. The significance of the difference is difficult to determine however. The fatigue lives of the corroded samples for both 17 kN and 15 kN can be shown to follow a log normal distribution with a high degree of significance. The 17 kN results shown in Table 10 exclude the results from specimens that did not fail from corrosion. The high significances (greater than 0.05) indicate lognormal distributions.

Table 10: One-Sample Kolmogorov-Smirnov Tests for log (fatigue life)

Load (kN)	*Stress (MPa)*	*N*	*Mean*	*Std. Deviation*	*Kolmogorov-Smirnov Z*	*Asymptotic Significance (2-tailed)*
15	124	11	5.9794	0.0401	0.627	0.826
17	140	8	5.7903	0.0401	0.386	0.998

Statistical analysis can predict failure rates for any likelihood from a given distribution, although prediction of the behaviour of low likelihoods requires a larger sample size in order to retain significance. However this does not address the assumptions that need to be made for any result here to be applied to a structural management plan; that the corrosion present on the specimens is representative of the corrosion that will be found on the aircraft fleet. Any fatigue life distribution will be related to the corrosion size distribution for the specific location on the aircraft. Determining a representative in-service corrosion distribution is extremely difficult. Teardown results and analysis of maintenance data have numerous difficulties that can make it difficult to determine a corrosion distribution with any degree of confidence. Any such distribution may also result in large numbers of specimens being required to accurately characterise the fatigue distribution in the areas of the distribution where corrosion sizes become significantly large.

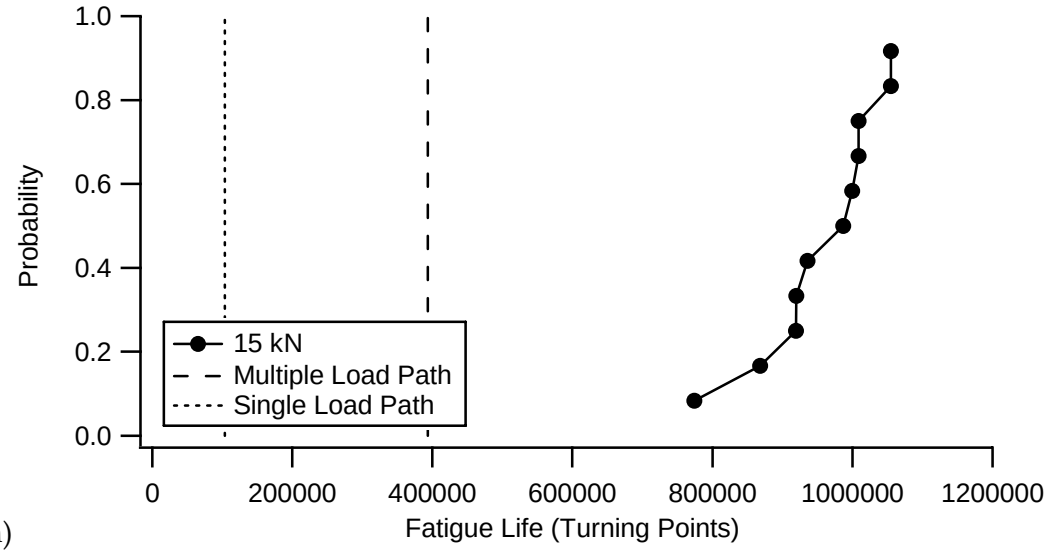

a)

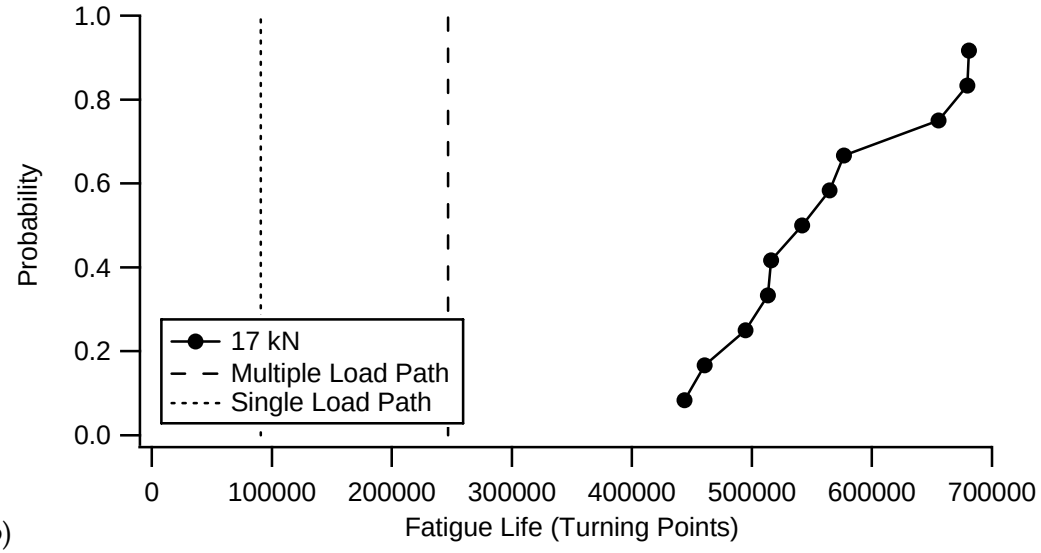

b)

Figure 17: Comparison of safe life estimates for single and multiple load path structure with fatigue results from corroded specimens for (a) 15 kN and (b) 17 kN peak load.

7. Comparison of ECS Predictions of the Effect of Corrosion on Safe Life

Fatigue lives predicted for the safe ECS values for both stress levels are shown in Figure 18. This figure also incorporates the crack initiation approach for P-3C SLAP. Threshold life values for both single and multiple load path structures were determined from the baseline fatigue tests using an interval between crack detection (crack reaching a size of 1.27 mm) and failure, provided by the FASTRAN model, Figure 14 and Figure 15. As can be seen, both at the low (15 kN), and the high (17 kN) stress levels corrosion pits, with a cross sectional area up to 80 µm (6,400 μm^2), will not result in failure prior to the threshold lives for both multiple and single load path structures.

Limitations of the ECS methodology prevent extrapolation outside of the bounds of measured behaviour due to the possibility of a change in mechanism. Additional work is required to more accurately characterise the upper end of the predicted safe life curves prior to any transition to service as very few data points occur in this area.

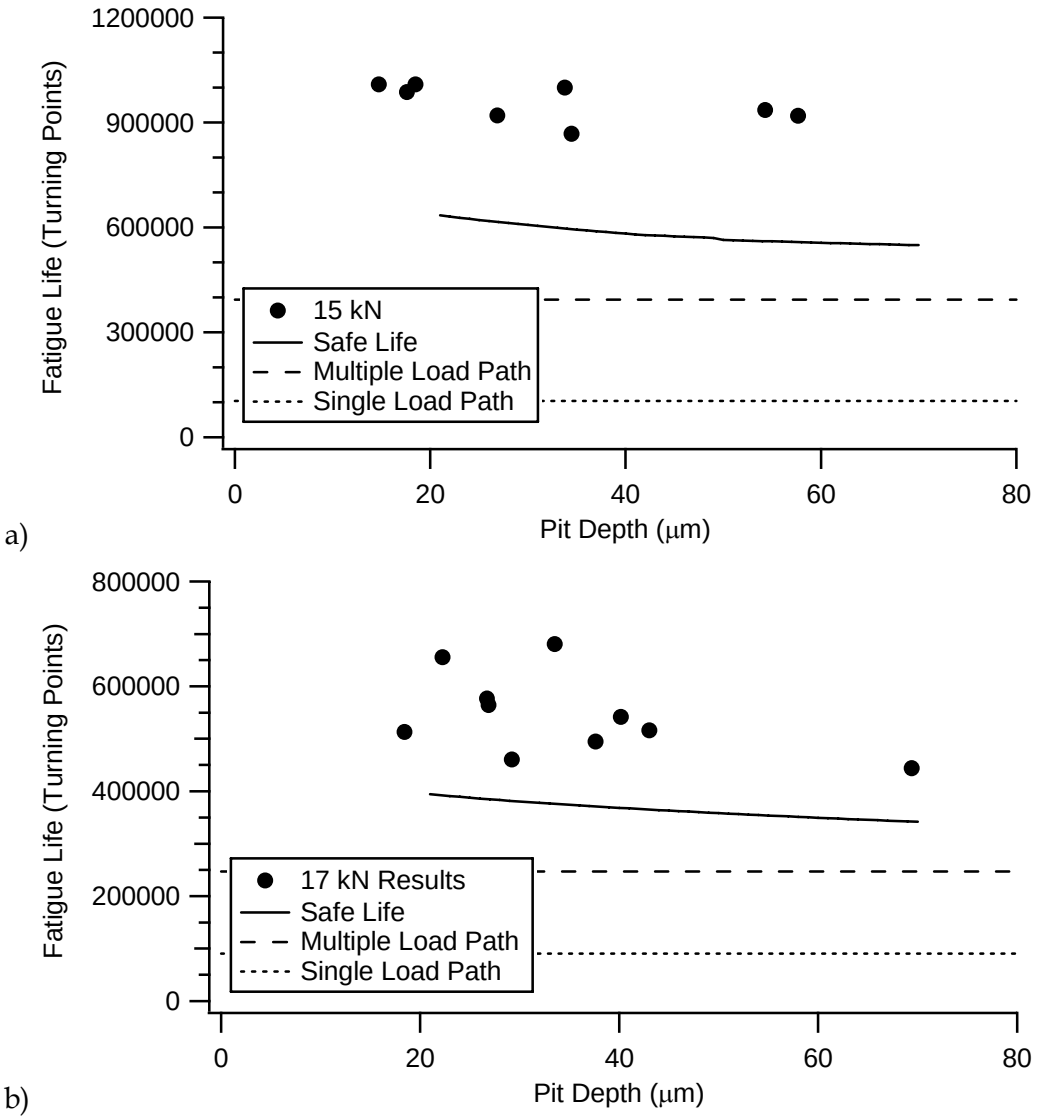

Figure 18: Comparison between the predicted failure lives due to corrosion with the threshold (safe life) values using Crack Initiation predictions for (a) 15kN and (b) 17kN peak load

The effect of corrosion on P-3C safe life was assessed using two methods: crack initiation (CI) and equivalent crack size (ECS). It should be noted that the CI method can be transferred between load spectra but requires the same corrosion distribution in service to produce a knockdown due to corrosion. In contrast, the ECS method can be used for different corrosion distributions, matching to an in-service distribution determined in the future, but is not readily transferable between load spectra. The ECS method has a significant advantage in that corrosion more severe than that used in its derivation can be easily incorporated into the model with a very small number of additional tests. CI models require the in-service corrosion distributions to be determined. The current RAAF practice of corrosion management makes this assessment difficult since corrosion is mostly removed (and thereby destroyed) once detected. The ECS methodology only requires the largest size of corrosion be determined. Characterisation of corrosion in service can allow the management of corrosion rather than its removal.

Neither model can account for a change in corrosion mode, i.e. from pitting to intergranular attack. It was apparent that the use of Alclad sheet prevented pits initiating close to the corners. The effect of the Alclad layer on baseline (un-corroded) lives has not been confirmed.

8. Conclusions

Following the investigation of the effect of corrosion on P-3C safe life it was concluded that:

8.1 Fatigue and Corrosion Behaviour

1. Pitting corrosion significantly reduced the fatigue life of the 7075-T6 material. In terms of the median life, this reduction ranged from 17% at 15 kN to 26% at 17 kN.
2. The mode of fatigue crack initiation differed between the corroded and uncorroded specimens. In the uncorroded material, fatigue cracks typically initiated from machining defects at hole corners. Fatigue cracks in the corroded material, conversely, initiated either from corrosion pits or, occasionally, from the Alclad layer.
3. The corrosion pits that initiated fatigue cracks had mean values of pit depth, width and area of 33.0 μm, 38.7 μm and 739 μm^2, respectively.

8.2 Equivalent Crack Size Modelling

4. Multiple linear regression showed that pit area had a statistically significant relationship with fatigue life. It was therefore used in subsequent modelling.
5. The ECS distribution was determined using FASTRAN. The mean ECS was 35.5 μm and was independent of load level.
6. A crack metric ratio (CMR) was determined and found to decrease as pit size increased. This differs from previous work on CMR, where it was observed to be independent of pit size. This is likely because of the much smaller size of pits (less than 100 μm depth) examined in the current work.
7. A 'safe' CMR relationship corresponding to a 1-in-1000 (0.001) failure probability was determined and used to calculate a 'safe' ECS. This was then used to calculate a fatigue life which was compared to the single load path and multiple load path life limits calculated according to the P-3C SLAP methodology. From this it was concluded that, for the range of pit size investigated, the P-3C safe life methodology was not invalidated.

8.3 Crack Initiation Modelling

8. A FASTRAN model was used to determine initial crack sizes (c_i) according to the P-3C SLAP methodology. It was found that corrosion increased the initiating crack size for both the 15 and 17 kN cases. This increase was of the order of approximately 0.2% or 4 μm, which is extremely small.

9. Corrosion reduced the time to crack initiation by approximately 26% for both the 15 and 17 kN load cases. However, the FASTRAN model predicted that crack propagation from crack initiation until final failure was effectively identical.
10. The above suggests, but does not prove, that corrosion alters the initiation phase of fatigue crack growth (here arbitrarily defined as crack lengths below 0.05" = 1.27 mm) while not affecting crack propagation. Therefore, it is critical that any models of fatigue crack development from corrosion damage accurately model the initiation of cracks.

8.4 General Conclusion

11. The crack initiation method requires the corrosion distribution to be representative of the in-service fleet while the ECS methodology only requires the corrosion to be bounded by the testing but cannot be used to extrapolate to other load spectra.
12. The pits examined in this work are relatively small. Larger pits, or a change in corrosion mechanism, are likely to invalidate the P-3C SLAP safe life methodology.

9. Acknowledgements

The authors would like to thank Phil Jackson for his guidance regarding the structural integrity methodology used in the P-3C SLAP program and for the samples tested here. They would also like to thank Emilio Matricciani for generating the loading spectrum used and Matthew Phillips for his provision of data and additional materials for testing. Finally, the assistance of Dr. Tony Trueman in developing the corrosion protocol was greatly appreciated.

10. References

1. Crawford, B.R., et al., *Structural Integrity Assessment of Corrosion in Aircraft Structures*. 2005, Melbourne: DSTO. DSTO-RR-0294.
2. Crawford, B.R., et al., *The EIFS distribution for anodised and pre-corroded 7010-T7651 under constant amplitude loading.* Fatigue and Fracture of Engineering Materials and Structures, 2005. **28**: p. 795-808.
3. Hartley, D., et al., *P-3C Service Life Assessment Program Australian Test Interpretation Report for the Empennage Test Articles*. 2005, Melbourne: DSTO. DSTO-TR-1856, 162.
4. Kinzie, R.C. *USAF Cost of Corrosion Maintenance*. in *Aging Aircraft*. 2002. San Francisco, California, USA: FAA/DOD/NASA.
5. Cole, G.K., G. Clark, and P.K. Sharp, *The implications of corrosion with respect to aircraft structural integrity*. 1997, Melbourne: DSTO. DSTO-RR-0102, 120.
6. Barter, S.A., P.K. Sharp, and G. Clark, *The failure of an F/A-18 trailing edge flap hinge.* Engineering Failure Analysis, 1994. **1**(4): p. 255-266.
7. Budnick, J. *NAVAIR Air Vehicle Corrosion Challenges*. in *Tri-Service Corrosion Conference*. 2003. Las Vegas: US Department of Defence.
8. Hoeppner, D.W., et al. *Corrosion and Fretting as Critical Aviation Safety Issues*. in *International Congress on Aircraft Fatigue*. 1995.

9. Peeler, D.T. and R.C. Kinzie. *Corrosion damage management and future outlook on corrosion prediction tools*. in *Aging Aircraft*. 2001.
10. Brooks, C.L., S. Prost-Domasky, and K. Honeycutt. *Corrosion is a Structural and Economic Problem: Transforming Metrics to a Life Prediction Method*. in *NATO RTO's Workshop 2 on Fatigue in the Presence of Corrosion*. 1998. Corfu, Greece,: NATO.
11. Teunisse, B., et al., *P-3C Service Life Assessment Program Australian Test Interpretation Report fro the USN Wing/Fuselage/Landing Gear Test Articles.* 2006.
12. Rudd, J.L. and T.D. Gray, *Quantification of Fastener-Hole Quality.* Journal of Aircraft, 1978. **15**(3): p. 143-147.
13. Manning, S.D. and J.N. Yang, *USAF Durability Design Handbook: Guidelines for the Analysis and Design of Durable Aircraft Structures*. 1985, Wright Patterson Air Force Base, Ohio, USA: United States Air Force. AFWAL-TR-83-3027.
14. Manning, S.D. and J.N. Yang, *Advanced Durability Analysis: Volume I, Analytical Methods*. 1987: Air Force Wright Aeronautical Laboratories. AFWAL-TR-86-3017.
15. Manning, S.D. and J.N. Yang, *Advanced Durability Analysis: Volume II, Analytical Predictions, Test Results and Analytical Correlations*. 1987: Air Force Wright Aeronautical Laboratories. AFWAL-TR-86-3017.
16. Manning, S.D. and J.N. Yang, *Advanced Durability Analysis: Volume V, Durability Analysis Software User's Guide*. 1987: Air Force Wright Aeronautical Laboratories. AFWAL-TR-86-3017.
17. Manning, S.D. and J.N. Yang, *Advanced Durability Analysis: Volume IV, Executive Summary*. 1987: Air Force Wright Aeronautical Laboratories. AFWAL-TR-86-3017.
18. Manning, S.D. and J.N. Yang, *Advanced Durability Analysis: Volume III, Fractographic Test Data*. 1987: Air Force Wright Aeronautical Laboratories. AFWAL-TR-86-3017.
19. Manning, S.D., *Durability Methods Development Volume VII - Phase II Documentation*. 1984, Air Force Wright Aeronautical Laboratories.
20. Mills, T., P.K. Sharp, and C. Loader, *The Incorporation of Pitting Corrosion Damage into F-111 Fatigue Life Modelling*. Research Report. 2002, Melbourne: DSTO. DSTO-RR-0237, 178.
21. Sharp, P.K., S.A. Barter, and G. Clark, *Localised Life Extension Specification for the F/A-18 Y470 X19 Pocket*. 2000, Melbourne: DSTO-AVD. DSTO-TN-0279.
22. Harter, J. *AFGROW Program*. [Web] 2003 [cited 2003 01/09/2003]; 4.0008.12.11:[Available from: http://afgrow.wpafb.af.mil/downloads/afgrow/techman.zip.
23. Harter, J. *AFGROW User's Guide*. 2003 [cited 2003 01/09/2003]; Available from: http://afgrow.wpafb.af.mil/downloads/afgrow/techman.zip.
24. Gumbel, E.J., *Elementare Ableitung der Momente für die Zahl der Überschreitungen*. Mitteilungsblatt Math. Statist, 1954. **6**: p. 164-169.
25. Turnbull, A., *Review of Modelling of pit propagation kinetics.* British Corrosion Journal, 1993. **28**(4): p. 297-308.
26. Marsh, G.P., *Statistical Study of Pit Propagation in Carbon Steel Under Nuclear Waste Disposal Conditions.* British Corrosion Journal, 1988. **23**(3): p. 157-164.
27. Laycock, P.J., R.A. Cottis, and P.A. Scarf, *Extrapolation of Extreme Pit Depths in Space and Time.* Journal of the Electrochemical Society, 1990. **137**: p. 64-69.
28. Ferguson, P.H., *Statistical Correlation of Pitting Measurements in Buried Iron Pipes.* 1993.
29. *E739-91(2004)e1 Standard Practice for Statistical Analysis of Linear or Linearized Stress-Life (S-N) and Strain-Life (ε-N) Fatigue Data*, in *ASTM Annual Book of Standards*. 2004, ASTM: Philadelphia.

30. Phillips, M., D. Hartley, and R. Amaratunga, *DSTO Coupon Testing Documentation in Support of the P-3 Service Life Assessment Program*. 2005, Melbourne: DSTO. DSTO-TR-1764.
31. Newman, J.C., *FASTRAN II - a fatigue crack growth structural analysis program*. 1992. NASA TM 104159.
32. *G1-90(1999)e1 Standard Practice for Preparing, Cleaning, and Evaluating Corrosion Test Specimens*, in *ASTM Annual Book of Standards*. 1999: Philadelphia. p. 15-21.
33. SPSS, *SPSS® Base 11.5 User's Guide*. 2002, Chicago: SPSS.
34. Pearson, S., *Initiation of Fatigue Cracks in Commercial Aluminum Alloys and the Subsequent Propagation of Very Short Cracks*. Engineering Fracture Mechanics, 1975. **7**(2): p. 235-247.

Appendix A: Fatigue Life Results

Table 11: Fatigue life results for corroded and uncorroded specimens

15 kN – Uncorroded		17 kN - Uncorroded	
Specimen ID	**Turning Points**	**Specimen ID**	**Turning Points**
A23	1077947	A28	688546
A26	1080411	A16	712635
A20	1128560	A15	722035
A30	1140783	A29	722441
A34	1140939	A19	734122
A32	1184118	A35	738331
A31	1194334	A13	744625
A33	1203853	A18	745885
A22	1209155	A17	758392
A25	1261686	A27	789651
A24	1365402	A14	791478
15 kN – Corroded		**17 kN - Corroded**	
Specimen ID	**Turning Points**	**Specimen ID**	**Turning Points**
39	774042	37	443953
A6	867935	34	460595
40	919356	A11	494665
30	919880	35	513413
38	935671	36	516124
A7	986751	A12	541586
A10	999835	A9	564671
A3	1008823	A1	576639
20	1008824	A5	655469
A2	1054666	A8	680876
32	1054762	A4	679475

Appendix B: Fractography Results

Table 12: Fractography results for corroded 7075 samples. Note that samples that did not fail due to corrosion are excluded from this table.

Corroded – 15 kN Maximum Load				
Specimen ID	**Pit Depth, (μm)**	**Pit Width, (μm)**	**Pit Area, (μm²)**	**Depth x Width (μm²)**
A6	37.5	31.6	478	1185
40	66.6	49.8	1665	3317
30	30.2	23.8	375	719
38	67.0	43.9	1484	2943
A7	7.6	40.4	124	307
A10	17.6	64.8	426	1141
A3	10	34.1	245	341
20	8.1	26.7	140	216
Corroded – 17 kN Maximum Load				
Specimen ID	**Pit Depth, (μm)**	**Pit Width, (μm)**	**Pit Area, (μm²)**	**Depth x Width (μm²)**
37	61.6	78.3	3349	4817
34	38.1	20.6	284	784
A11	46.0	30.8	968	1418
35	9.8	34.3	209	336
36	51	36.2	817	1846
A12	48.2	33.5	744	1615
A9	35.2	20.5	397	722
A1	20.1	35.4	435	712
A5	6.5	13.9	56	90
A8	47.6	23.6	623	1123

DEFENCE SCIENCE AND TECHNOLOGY ORGANISATION
DOCUMENT CONTROL DATA

1. PRIVACY MARKING/CAVEAT (OF DOCUMENT)

2. TITLE

Assessment of the Effect of Pitting Corrosion on the Safe Life Prediction of the P-3C

3. SECURITY CLASSIFICATION (FOR UNCLASSIFIED REPORTS THAT ARE LIMITED RELEASE USE (L) NEXT TO DOCUMENT CLASSIFICATION)

Document (U)
Title (U)
Abstract (U)

4. AUTHOR(S)

A. Shekhter, C. Loader, W. Hu and B. R. Crawford

5. CORPORATE AUTHOR

DSTO Defence Science and Technology Organisation
506 Lorimer St
Fishermans Bend Victoria 3207 Australia

6a. DSTO NUMBER	6b. AR NUMBER	6c. TYPE OF REPORT	7. DOCUMENT DATE
DSTO-TR-2080	AR-014-063	Technical Report	December 2007

8. FILE NUMBER	9. TASK NUMBER	10. TASK SPONSOR	11. NO. OF PAGES	12. NO. OF REFERENCES
eg: 510/207/0128	03-111	DGTA	35	34

13. URL on the World Wide Web

http://www.dsto.defence.gov.au/corporate/reports/DSTO-TR-2080.pdf

14. RELEASE AUTHORITY

Chief, Air Vehicles Division

15. SECONDARY RELEASE STATEMENT OF THIS DOCUMENT

Approved for public release

OVERSEAS ENQUIRIES OUTSIDE STATED LIMITATIONS SHOULD BE REFERRED THROUGH DOCUMENT EXCHANGE, PO BOX 1500, EDINBURGH, SA 5111

16. DELIBERATE ANNOUNCEMENT

No Limitations

17. CITATION IN OTHER DOCUMENTS Yes

18. DSTO RESEARCH LIBRARY THESAURUS http://web-vic.dsto.defence.gov.au/workareas/library/resources/dsto_thesaurus.htm

P3C aircraft, Orion aircraft, Corrosion, Pitting, Fatigue Tests (Mechanics) or Fatigue life, Service life (Engineering), Aluminium alloy 7075-T6

19. ABSTRACT

This report presents the results of an experimental programme aimed at assessing the implications of pitting corrosion damage on P-3C safe lives calculated using the methods developed in the P-3C Service Life Assessment Program, the Equivalent Crack Size method and the Crack Initiation method. The results of both of these methods were that, for the pitting corrosion distribution used, the safe life prediction was not invalidated by corrosion. However, larger corrosion pits or a change of corrosion mechanism may invalidate safe life predictions.